**The EMBO Journal** Vol.17 No.20 pp.5855–5867, 1998

# KIF2β, a new kinesin superfamily protein in non-neuronal cells, is associated with lysosomes and may be implicated in their centrifugal translocation

**Niovi Santama[1,2,3], Jacomine Krijnse-Locker[1], Gareth Griffiths[1], Yasuko Noda[4], Nobutaka Hirokawa[4] and Carlos G.Dotti[1,3]**

[1]Cell Biology Programme, European Molecular Biology Laboratory, Heidelberg D-69012, Germany and [4]Department of Anatomy and Cell Biology, Faculty of Medicine, University of Tokyo, Tokyo 113, Japan

[2]Present address: University of Cyprus and Cyprus Institute of Neurology and Genetics, PO Box 3462, 1683 Nicosia, Cyprus

[3]Corresponding authors
e-mail: dotti@EMBL-Heidelberg.de and santama@earth.ns.ucy.ac.cy

**Lysosomes concentrate juxtanuclearly in the region around the microtubule-organizing center by interaction with microtubules. Different experimental and physiological conditions can induce these organelles to move to the cell periphery by a mechanism implying a plus-end-directed microtubule-motor protein (a kinesin-like motor). The responsible kinesin-superfamily protein, however, is unknown. We have identified a new mouse isoform of the kinesin superfamily, KIF2β, an alternatively spliced isoform of the known, neuronal kinesin, KIF2. Developmental expression pattern and cell-type analysis *in vivo* and *in vitro* reveal that KIF2β is abundant at early developmental stages of the hippocampus but is then downregulated in differentiated neuronal cells, and it is mainly or uniquely expressed in non-neuronal cells while KIF2 remains exclusively neuronal. Electron microscopy of mouse fibroblasts and immunofluorescence of KIF2β-transiently-transfected fibroblasts show KIF2 and KIF2β primarily associated with lysosomes, and this association can be disrupted by detergent treatment. In KIF2β-overexpressing cells, lysosomes (labeled with anti-lysosome-associated membrane protein-1) become abnormally large and peripherally located at some distance from their usual perinuclear positions. Overexpression of KIF2 or KIF2β does not change the size or distribution of early, late and recycling endosomes nor does overexpression of different kinesin superfamily proteins result in changes in lysosome size or positioning. These results implicate KIF2β as a motor responsible for the peripheral translocation of lysosomes.**

*Keywords*: kinesins/lamp-1,2/lysosomes/microtubules/motor proteins

## Introduction

Cell morphogenesis and differentiation entail centrifugal elongation of membranes to form extended tubular structures and bidirectional intracellular membrane and organelle movement. Many of these translocations require the presence of an intact microtubule (MT) network, are ATP-dependent and are mediated by MT-based motor proteins that power both anterograde (kinesin and kinesin-superfamily proteins) and retrograde (dynein and dynein-superfamily proteins) movement (reviewed by Bloom and Endow, 1994, 1995; Dillman *et al.*, 1996; Hirokawa, 1996a, 1998; Ogawa and Mohri, 1996).

In neurons, the different metabolic demands and requirements for macromolecules of the distinct neuronal domains (somatodendritic or axonal) necessitate a tightly controlled system for efficiently transporting and positioning organelles, vesicles, membrane and other proteins within the cell with different patterns of trafficking in axons versus dendrites. Hence, it is of interest to unravel the MT-based machinery that is involved in neuronal differentiation and polarized targeting, and to analyze the precise function of motor proteins, and their interactions, biochemical properties and ligands.

We undertook a screen to identify novel motor proteins in mouse that are differentially expressed during distinct stages of neuronal differentiation and to analyze their possible role in intracellular organelle transport. There is a wealth of genetic, molecular biological and immunological data that has led to the identification of ~100 kinesin-like proteins, present in essentially all the major eukaryotic phyla (reviewed in Bloom and Endow, 1995; Moore and Endow, 1996), >30 in mouse alone (Hirokawa 1996a,b, 1998; Nakagawa *et al.*, 1997). Although not proven, the consensus suggests that kinesin superfamily proteins (KIFs) can have specific interactions with their cargoes through their non-conserved, variable domains and this determines the type of the membrane-bound cargo for each member. The sheer number of different members of the kinesin superfamily in each organism, increased by the presence of multiple isoforms and the potential for combinatorial heteromerization can provide endless possibilities for cargo selectivity and multiplies the functional complexity of the motor machinery.

The identification of distinct cargoes for distinct members, an essential step in elucidating the motor function, is emerging, however, more slowly for interphase or neuronal KIFs, than for meiotic or mitotic kinesins (Moore and Endow, 1996; Walczak and Mitchison, 1996). Such cargoes include organelles and vesicles: mitochondria are the cargo of murine KIF1B (Nangaku *et al.*, 1994), its isoform KIF1A transports synaptic vesicle precursors along the axon (Okada *et al.*, 1995), while the membrane-bound organelles transported by the heterotrimer KIF3A–KIF3B–KAP3 (Yamazaki *et al.*, 1995, 1996; Scholey, 1996) as well as the cargo of KIF4 (Sekine *et al.*, 1994) or KIF2 (Noda *et al.*, 1995; Morfini *et al.*, 1997) have not yet been conclusively characterized.

The possible role of kinesin and dynein-like motor

proteins in the movement and positioning of late endocytic organelles has been well documented by diverse evidence. Lysosomes accumulate centrally, suggesting an interaction with microtubules via dynein (Herman and Albertini, 1984; Matteoni and Kreis, 1987; Lin and Collins, 1992; McGraw *et al.*, 1993; Oda *et al.*, 1995) but they can also move towards the cell periphery in a kinesin-dependent manner (Hollenbeck and Swanson, 1990; Feiguin *et al.*, 1994; Nakata and Hirokawa, 1995). Experimental protocols that depolymerize MTs or disturb the dynein–kinesin balance have a profound effect on lysosome morphology and positioning. Examples include nocodazole-induced dispersion of lysosomes (Matteoni and Kreis, 1987), the dramatic re-distribution of lysosomes upon cytoplasmic acidification/alkalinization or overexpression of dynamitin or elimination of cytoplasmic dynein expression (Heuser, 1989; Parton *et al.*, 1991; Burkhardt *et al.*, 1997; Harada *et al.*, 1998), anti-kinesin antibody-induced inhibition of radial lysosomal movement (Hollenbeck and Swanson, 1990) and blocking of anterograde lysosome transport by mutations in the ATP-binding domain of overexpressed kinesin (Nakata and Hirokawa, 1995). Moreover, kinesin-mediated, microtubule-dependent, directional migration of host lysosomes towards the site of parasite attachment is critical for effective *Trypanosoma cruzi* invasion in mammalian cells (Tardieux *et al.*, 1992; Rodriguez *et al.*, 1996).

This collective evidence implicates a role for MT-based motor machinery in the formation of lysosomes, suggesting that aberrant morphology and localization of these organelles may be caused by a perturbation of the organelle and plus/minus-end-directed motor interaction. However, the native specific KIF(s) responsible for centrifugal lysosomal movement has not yet been identified.

Here we identify a novel kinesin superfamily protein, KIF2β, which is an isoform of KIF2. We show that the two isoforms KIF2 and KIF2β are differentially expressed during neuronal differentiation in the hippocampus, both *in vivo* and *in vitro*, and while the expression of KIF2 is neuron-specific, KIF2β is expressed in mitotic cell types such as astrocytes and fibroblasts. KIF2β is specifically associated with lysosomes and its overexpression induces these organelles to become significantly enlarged and redistribute from their usual perinuclear location towards the cell periphery. These findings provide, to our knowledge, the first direct, *in vivo* identification of a functional association of lysosomes with a distinct, native member of the kinesin superfamily.

## Results

### *Isolation and sequencing of KIF2β cDNA*

We first observed the possible existence of a KIF2-like isoform when we carried out a reverse-transcription polymerase chain reaction (RT–PCR) of E15 embryonic mouse hippocampal mRNA, using a set of primers, designed to amplify part of the motor domain region of KIF2 (set 1, see Materials and methods). This reaction revealed a product with the expected mol. wt for the KIF2 amplified region and a second, smaller mol. wt product (Figure 1A). In order to determine the identity of the smaller product, we carried out a second RT–PCR of E15 mRNA using a set of primers designed to amplify the entire open reading frame (ORF) of KIF2 (set 2, see Materials and methods). This resulted in a product with the correct mol. wt for the primers used (2189 bp of KIF2) as well as a second, smaller-sized band (Figure 1B). The two PCR products were directly cloned in the T/A cloning vector, and analyzed for insert size with *Eco*RI restriction digests, and the two different-sized inserts were subjected to full-length sequencing of both strands using primers to overlapping fragments. The cDNA sequence of the large band corresponded to the known mouse KIF2 sequence (data not shown; Aizawa *et al.*, 1992). The sequence of the smaller product revealed the ORF of a novel KIF2-like isoform which we name KIF2β (Figure 2A; DDBJ/EMBL/GenBank accession No. Y15894).

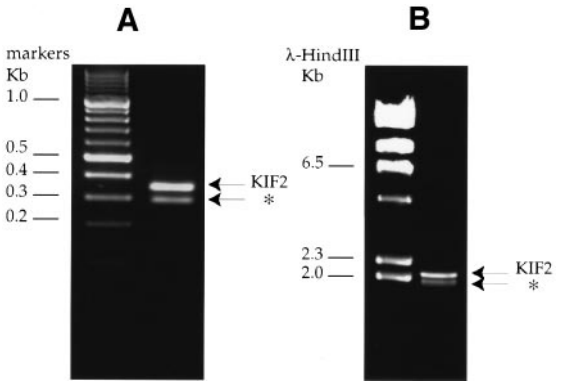


**Fig. 1.** Identification and cloning of a novel KIF2-like isoform. (**A**) RT–PCR on E15 cDNA, using an internal set of primers designed to amplify the region of KIF2 included between nucleotides 709 and 1048 (set 1, see Materials and methods) reveals, in addition to the expected product of 339 bp, a second, smaller mol. wt band (asterisk). (**B**) For cloning of the second, unknown product, RT–PCR was repeated with E15 cDNA, using a set of primers (set 2, see Materials and methods) designed to amplify the complete ORF of KIF2 (2189 bp). It resulted in the simultaneous amplification of a slightly smaller product (asterisk) which was cloned and sequenced and proved to be the ORF of a novel isoform, termed KIF2β (see Figure 2).

KIF2β has 171 nucleotides (57 amino acids, aa) less than KIF2, otherwise the two isoforms are identical (except for an alanine instead of a glycine at position 106). The missing amino acids are in non-conserved, variable domains of the protein and distributed in two regions: one (19 aa) is upstream and the other (38 aa) is downstream of the conserved protein motor domain (Figure 2B).

The motor domain of KIF2β is centrally localized and contains the conserved motifs typical of kinesin superfamily proteins (Trayer and Smith, 1997). In addition, it harbors an RKTK sequence which resembles sufficiently the nuclear localization (NLS) motif K-R/K-X-R/K (Chelsky *et al.*, 1989; Mattaj and Englmeier, 1998) and could possibly function as an NLS (Figure 2A).

From the sequence, it is clear that KIF2β and KIF2 are differentially spliced products of a common primary transcript. Some of the murine KIFs that have been identified to date appear to exist in isoforms but those are derived from distinct genes with extensive sequence similarity (KIF1A and B, KIF3A and B, and KIF5A–C; summarized in Nakagawa *et al.*, 1997). In contrast, KIF2β and KIF2 appear to be a subfamily of spliced isoforms. This may be a common pattern in other organisms, given the recent identification of HK2 (human kinesin 2;

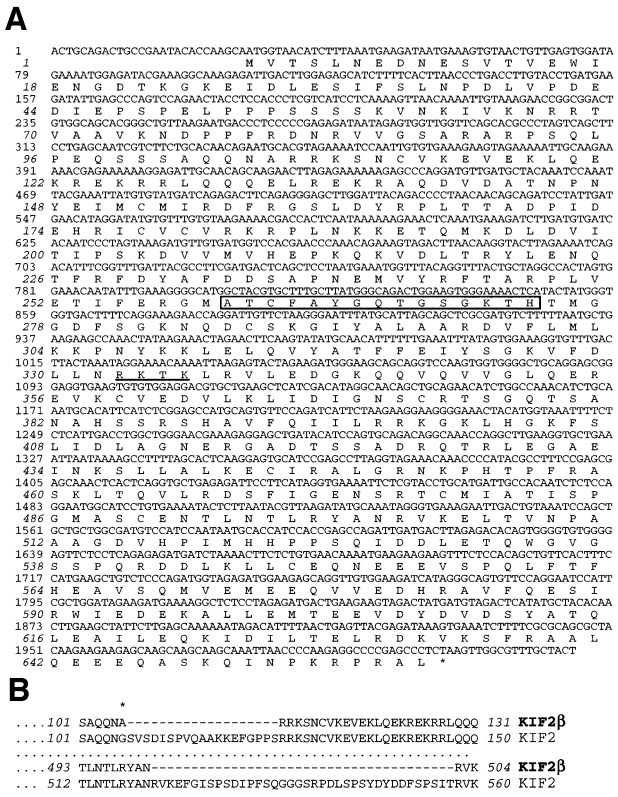


**Fig. 2.** (**A**) Nucleotide and protein sequence of the novel isoform KIF2β. The complete ORF of KIF2β is 171 nucleotides shorter but otherwise completely identical to KIF2. Compared with KIF2, KIF2β lacks two internal, non-contiguous, sequences, one in the upstream variable domain (nucleotides 823–879 of KIF2) and the other in the downstream variable domain (2065–2178 in KIF2), respectively. The positions of these deletions, in respect to KIF2, are shown in detail at the bottom panel. The motor domain is centrally localized, as in KIF2 (Noda *et al.*, 1995). The ATP-binding domain is boxed and a putative nuclear localization signal, within the motor domain, is underlined. The sequence of KIF2β was deposited to the DDBJ/EMBL/GenBank database with accession No. Y15894. (**B**) Protein sequence alignment of KIF2β and KIF2 over the regions of difference. The KIF2β protein lacks two short regions of 19 aa (amino acid residues 107–125 of KIF2) and 38 aa (residues 521–557). Residue 106 of KIF2β is an alanine (asterisk), compared with a glycine at the same position in KIF2.

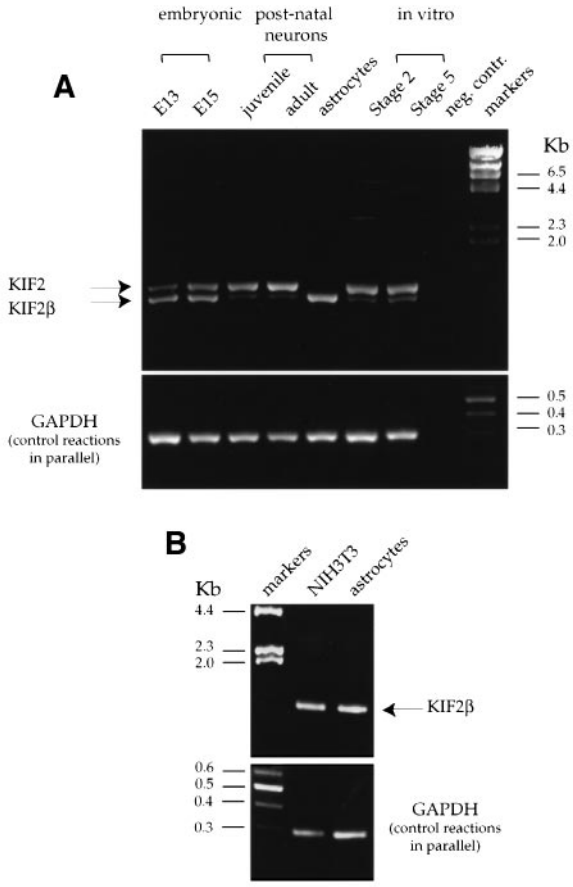


**Fig. 3.** (**A**) Comparative analysis by RT–PCR of the pattern of expression of the two KIF2-like isoforms during distinct stages of differentiation of the hippocampus *in vivo* and of hippocampal cultures *in vitro*. RT–PCRs were carried out with a set of primers (set 4, see Materials and methods) generating different-size products, diagnostic for KIF2 and KIF2β (top panel). cDNA was constructed from identical amounts of RNA, isolated from the hippocampus of E13 and E15 mouse embryos, juvenile (2.5 weeks) and adult (3 months) animals as well as from hippocampal neurons differentiating *in vitro* and corresponding to stage 2 (unpolarized) and stage 5 (fully mature neurons), as per Dotti *et al.* (1988) and from pure, proliferating, astrocyte cultures from newborn animals. The negative control reaction consisted of a mock reverse transcription reaction (no reverse transcriptase was added) with E13 RNA. Equivalent reactions amplifying mouse GAPDH (oligo set 5), were carried out in parallel with the same amounts of cDNA as test reactions and used as internal standards (bottom panel). (**B**) Expression of the KIF2-like isoforms in NIH 3T3 mouse fibroblasts. RT–PCR as in (A), reveals that only the KIF2β isoform is expressed in the mouse NIH 3T3 fibroblast cell line [a sample from astrocyte cDNA, identical as in (A), is run alongside for qualitative and quantitative comparison]. Control reactions for GAPDH (bottom panel).

Debernardi *et al.*, 1997) which is >90% similar to mouse KIF2 and a shorter form, $HK2_S$, containing a 57 bp deletion in its ORF, that is identical to the first of the two deletions in KIF2β, reported here. However, $HK2_S$ does maintain the second region of 113 bp that is missing in KIF2β. KIF2/2β also show high sequence similarity, particularly within the motor domain, with other central motor domain KIFs: MCAK from Chinese hamster (Wordeman and Mitchison, 1995), XKCM1 of *Xenopus* (Walczak *et al.*, 1996) and rat rKRP2 (Sperry and Zhao, 1996), although it is not clear whether these proteins also exist in multiple isoforms. Despite the sequence similarity it appears that the above proteins are not the true corresponding homologues of mouse KIF2 (or KIF2β) (Walczak *et al.*, 1996).

### *KIF2 and KIF2β are differentially expressed during differentiation of hippocampal cells in vivo and in vitro*

In order to start characterizing the novel KIF, we were interested in determining the pattern of expression of the two KIF2 isoforms during hippocampal neuronal development. Equivalent amounts of cDNA were constructed from isolated hippocampi of E13 and E15 mouse embryos, juvenile and adult animals as well as from cultures of hippocampal neurons differentiating *in vitro* and corresponding to stage 2 or 3 (unpolarised) and stage 5 (fully mature neurons), as described previously by Dotti *et al.* (1988). cDNA isolated from all these sources was subjected to PCR using a set of primers (set 4, see Materials and methods), generating products diagnostic for KIF2 and KIF2β. Figure 3A shows the result of this analysis. Early in the development of the hippocampus,

KIF2β is the predominant isoform, while by E15 both KIF2 and KIF2β are expressed at similar levels. After birth however, there is a clear change in the molar ratio in favor of KIF2, which is maintained in the adult. Similarly to the results obtained from hippocampi (tissue) mRNA, RT–PCR of mRNA obtained from mouse hippocampal neurons, maintained in culture for 3 (stage 2–3) and 15 days (stage 5), and corresponding developmentally to post-natal animal stages, resulted in the predominance of KIF2 over KIF2β. Given that a small proportion of glial cells are present in the hippocampal cultures and also that glial cells are present in the hippocampus *in situ*, we performed RT–PCR using mRNA obtained from a 100% pure astrocytic primary culture. In the material from these cells only the band corresponding to KIF2β was detected (Figure 3A).

It is known that in E13 hippocampus different cell types are present: glia (radial astroglia and microglia), differentiating neurons and neuroepithelium that will give rise to neuron and glia progenitor cells. Hence, at this early stage, the abundant KIF2β product that we detected could be derived from any of these cell types or be of purely glial origin. In any case, after birth, KIF2β becomes downregulated in hippocampal cells, both *in vivo* and *in vitro*, and is only, or mainly, expressed in the non-neuronal astrocytes (Figure 3A). The paucity of KIF2β *in vitro* at later stages and in *in situ* hippocampal cells, compared with the abundance of KIF2β in the mRNA from the pure astrocyte culture, could be explained by the low percentage of glial cells in hippocampal cultures and post-natal isolated hippocampi. On the basis of our results, we cannot rule out that KIF2β continues to be expressed in differentiated neurons. However, if this is the case, KIF2β is at most only a minor isoform, compared to KIF2. Similarly to glia, NIH 3T3 fibroblasts, another non-neuronal type, also express KIF2β exclusively (Figure 3B). The results of the RT–PCR analysis on the expression of the two KIF2-like isoforms were also corroborated by Western blot analysis (see Figure 5a later in the results section).

In conclusion, our analysis suggests that KIF2 is the main or exclusive neuronal isoform, while KIF2β is mainly, or solely, expressed in non-neuronal cells that retain the ability to divide.

### *Intracellular distribution of KIF2 and KIF2β in neurons and fibroblasts*

To analyze the intracellular distribution of KIF2β using polyclonal and monoclonal antibodies against KIF2 (Noda *et al.*, 1995) we performed indirect immunofluorescence microscopy in cultures of hippocampal neurons and NIH 3T3 fibroblasts. It is not possible to raise KIF2β-specific antibodies that do not recognize KIF2, as KIF2β lacks 57 aa but is otherwise identical to KIF2. However, given the pattern of isoform expression, the antiserum used is expected to recognize KIF2 in neurons while it will specifically recognize KIF2β in fibroblasts, as this is the only isoform expressed in this cell type (see Figure 5a).

In neurons, a fine punctate cytosolic staining, extending to the cell body and the proximal part of the thicker processes, was detected (Figure 4A). In interphase fibroblasts we also observed a very fine punctate labeling extending to both nucleus and cytoplasm (Figure 4B).

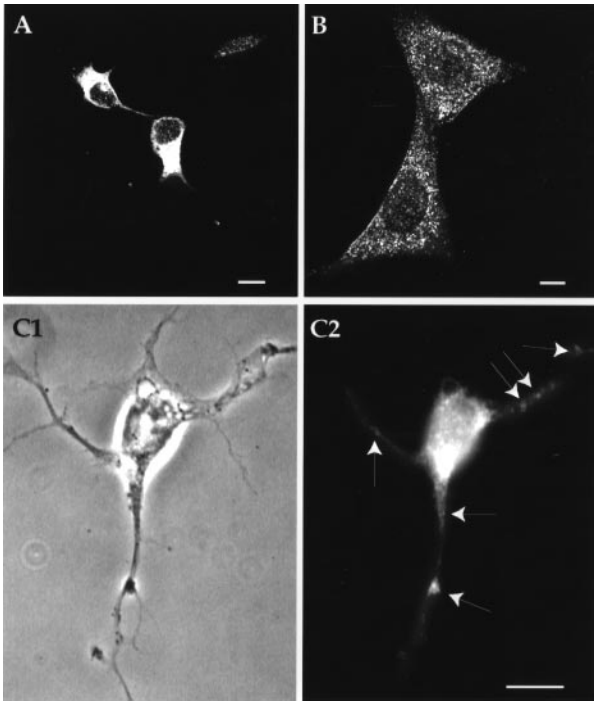


**Fig. 4.** Anti-KIF2/2β immunoreactivity revealed by immunofluorescence in cultured hippocampal neurons and NIH 3T3 fibroblasts using polyclonal anti-KIF2 antiserum (A and B) and immunolocalization of myc-KIF2 in transiently transfected hippocampal neurons (C1, and C2). (**A**) KIF2-labeled hippocampal neurons and one glial cell (upper right corner); (**B**) KIF2 immunoreactivity in mouse interphase fibroblasts; (**C1**) phase contrast of a hippocampal neuron in culture that was transfected with pSVmycKIF2; (**C2**) equivalent anti-myc immunofluorescence, revealing a dense, punctate, vesicular-like staining which is mainly perinuclear but also localized in some of the processes, at a distance from the cell body (arrows). Scale bar in confocal micrographs (A and B): 6 μm; in light micrographs (C1 and C2): 10 μm.

This pattern is typically observed for interphase cells when antisera that recognize cytoplasmic KIFs are used (discussed by Bloom and Endow, 1994) and was not very informative as we could not resolve the distinct cytoplasmic compartment with which labeling was associated. Interestingly, using the monoclonal anti-KIF2 antibody, labeling was also detected at the poles of the mitotic spindle in dividing fibroblasts (data not shown).

### *Overexpressed KIF2 and KIF2β associate with mature lysosomes and the nucleus*

To gain some insight into the intracellular distribution and possible role of these kinesin-like proteins, KIF2 was overexpressed in cultured hippocampal neurons. Cells were transfected by a modified calcium/phosphate precipitation method (see Materials and methods) and immunostained with anti-myc antibody. In neurons, mycKIF2 overexpressed protein appeared mainly concentrated in small vesicular structures densely scattered in the cell body mainly juxtanuclearly, in the initial segments of the processes, both of the axon and dendrites (Figure 4, C1 and C2), similar to the results obtained with anti-KIF2 immunofluorescence; but also in some larger vesicular structures localized at some distance along the processes (arrows in Figure 4, C2). Next we repeated the transfections of tagged KIF2 or KIF2β proteins in NIH 3T3 mouse fibroblasts, where we continued our analysis taking advant-

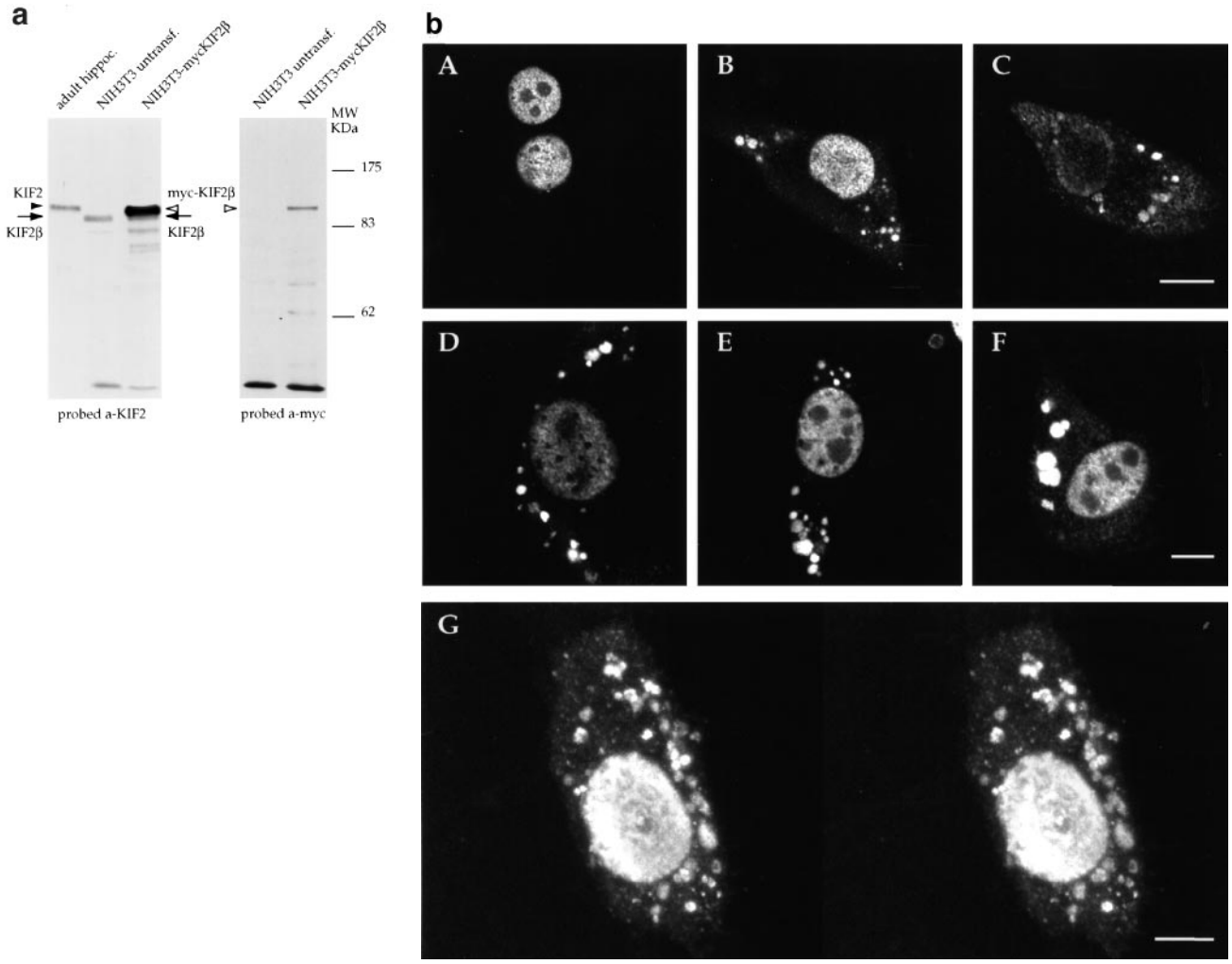


**Fig. 5.** (**a**) Western immunoblotting on equivalent total protein fractions from mouse extracts. The left panel was probed with anti-KIF2 polyclonal antiserum and the right panel with anti-myc monoclonal antibody. (Left panel) KIF2 (black arrowheads) and KIF2β (arrows) can be detected respectively in a hippocampal sample derived from adult mouse (3 months) and NIH 3T3 cultures (lanes 2 and 3). In lane 3 (NIH 3T3 transfected with myc-KIF2β) an additional, prominent band is detected, corresponding to the tagged KIF2β protein (white arrowheads; the slightly higher mol. wt is due to an additional 13 N-terminal amino acids, including the myc epitope, that contribute 1334 Da). (Right panel) The prominent band is confirmed as immunoreactive to the anti-myc monoclonal antibody and is uniquely detected in the sample derived from transfected fibroblasts. (**b**) A gallery of confocal micrographs showing immunolocalization of myc-tagged KIF2β in transiently transfected NIH 3T3 mouse fibroblasts. In transfected cells, anti-myc immunolabeling was typically detected (A) in the nucleus, excluding nucleoli; (B) in both nucleus and in small (0.25–0.5 μm) cytoplasmic, vesicular-like structures, localized in the cytoplasmic periphery; (C) occasionally, a diffuse, fine, punctate cytoplasmic labeling was also detected in addition to the vesicular structures; (D and E) the organization of the immunopositive vesicular structures appeared dynamic, as their size exhibited great heterogeneity (0.25–1.5 μm). They were dispersed at a distance from the nucleus and bordering the plasma membrane; (F) very large vesicular structures (up to 3 μm) were regularly observed. Identical results were obtained in transfections with myc-KIF2. Scale bars in confocal micrographs: 11 μm for (A–C) and 5 μm for (D–F). (G) Stereo projection of a reconstruction of a stack of serial confocal sections through a transfected, KIF2β-expressing fibroblast, revealing immunolabeling of the nucleus, striking cytoplasmic vesicular structures and also a diffuse punctate pattern. Observe the ring-like appearance of staining in many of the vesicles. Scale bar of stereo projection: 5 μm.

age of the ease of routine transfections in this cell type compared with neurons, whose survival suffered from the toxic effects of the transfection reagents.

Western blot analysis confirmed high levels of KIF2β expression in NIH 3T3 fibroblasts following transfection (Figure 5a). A prominent, immunoreactive band that is both KIF2- and myc-immunopositive was uniquely detected in transfected cells, in addition to the native KIF2β (Figure 5a, compare left and right panels). To confirm that the anti-myc antibody was a reliable indicator of KIF2 (or 2β) expression for immunofluorescence staining, double-labeling experiments were carried out using the two antisera. This revealed an exact correspondence of anti-myc and anti-KIF2 staining in mycKIF2- or 2β-transfected NIH 3T3 (data not shown).

In transfected NIH 3T3 cells, anti-myc immunolabeling was typically detected in the nucleus, excluding nucleoli (Figure 5b, A) and in prominent cytoplasmic, vesicular-like structures (Figure 5b, B–G). Occasionally, a diffuse, fine, punctate cytoplasmic labeling was also detected in addition to the vesicular structures (Figure 5b, B). The organization of the immunopositive vesicular structures appeared dynamic, as their size exhibited great heterogeneity (usually from 0.25–1.5 μm and occasionally up to 3 μm), and seemed unrelated to the presence or absence or the level of nuclear staining (Figure 5b, B–G). Figure

5b, G shows a stereo reconstruction of a series of optical confocal sections through a transfected fibroblast, illustrating that in most of the labeled vesicles, staining decorates the peripheral rim of the vesicular structure and not its interior. Identical results were obtained with the use of myc-tagged KIF2- or KIF2β-bearing plasmids and thus, we refer to KIF2/2β in the description of subsequent experiments. It is notable that in our transfections we did not obtain the spindle pole labeling observed in dividing fibroblasts stained with the monoclonal anti-KIF2 antibody, although as mentioned above, prominent nuclear anti-myc labeling was observed in transfected interphase fibroblasts.

Nuclear labeling and immunopositive cytoplasmic vesicles, like those observed in transfected cells, were also detected following nuclear microinjection of plasmid pSVmKIF2 or 2β in NIH 3T3 (R.Saffrich, EMBL; data not shown).

As a control, to demonstrate that the intracellular targeting of the overexpressed protein in our particular mammalian expression system is not artifactually influenced by the type of the in-frame 5′ tag, we carried out transfections with his-tagged KIF2 (pSVhisKIF2) and obtained the same characteristic pattern of nuclear plus cytoplasmic vesicular staining (data not shown). In addition, to demonstrate that the transfection vector pSVmyc1.0 is a valid tool for the localization of tagged proteins in mammalian cells, an unrelated protein, human ribosomal protein L22, with a distinct subcellular localization, was tested. Myc-tagged L22 localized appropriately, both to the nucleolus and to the ribosomes in the cytoplasm (data not shown). To rule out a non-specific cytoplasmic sequestering or localization of overexpressed motor proteins due, for example, to interaction of the MT-binding motor domain with microtubules, we also transfected cells with two other myc-tagged kinesin-like proteins, *Xenopus* XKLP1 (a chromosome-binding kinesin; Vernos *et al.*, 1995) and a new, cytoplasmic mouse KIF (E.Piddini and C.G.Dotti, unpublished results). We observed that each kinesin localized appropriately and uniquely to its corresponding subcellular compartment: XKLP1 to the nucleus, excluding nucleoli, and the novel KIF to ER membranes (data not shown).

Next we analyzed the identity of the KIF2 or 2β-immunopositive vesicular structures in NIH 3T3 transfected cells. Given their peripheral distribution and round shape we hypothesized that these structures may be of endocytic origin: early endosomes, recycling endosomes, late endosomes or lysosomes, the contents of which are transported, both *in vivo* and *in vitro* in a microtubule-mediated fashion (Aniento *et al.*, 1993; Oda *et al.*, 1995). To discern between these possible localizations, transfected cells were subjected to double immunofluorescence using anti-myc and antibodies which serve as markers for early, recycling and late endocytic structures. The results of these experiments are shown in Figure 6. KIF2/KIF2β and eea1, a marker for early endosomes (Mu *et al.*, 1995), did not colocalize (Figure 6A). To analyze whether the KIF2/KIF2β-positive structures corresponded to endosomes involved in plasma membrane recycling, transfected cells were incubated for short and longer times with fluorescein-conjugated transferrin (Tf). Tf internalized for short times appeared uniformly distributed in both transfected and non-transfected cells and after a longer incubation time Tf-labeled structures were mostly positioned juxtanuclearly, suggesting that KIF2/2β overexpression does not have an effect on the normal endocytic trafficking (Figure 6B and C, green labeling). Similar to the lack of colocalization with eea1, internalized Tf did not co-localize with KIF2/KIF2β either (Figure 6B and C), suggesting absence of labeling in early endosomes and the recycling compartment (late endosomes are not usually labeled via Tf internalization). Consistently, no co-localization was observed in double-labeling experiments using anti-myc and an antibody against the Tf receptor (Figure 6D). Finally, late endosomes and the pre-lysosomal compartment, labeled with two independent antisera against different domains of the cation independent mannose 6-phosphate receptor (CI-MPR; see Materials and methods) were also negative for KIF2/2β (Figure 6E and F).

Having excluded early, recycling and late endosomes, we then examined the final compartment of the endocytic pathway, mature or secondary lysosomes (where MRPs are not present; Geuze *et al.*, 1988; Griffiths *et al.*, 1988). Indeed, using antibodies to the lysosomal markers, the lysosome-associated membrane proteins, lamp-1 (Figure 7A) and lamp-2 (data not shown), we were able to demonstrate that the KIF2- or KIF2β-associated vesicles in transfected cells were lysosomes. In transfected cells, cytoplasmic anti-myc and anti-lamp-1 staining were coincident (Figure 7A, A3 and B3 for overlays). In the transfected cells shown as an example in Figure 7A, it is possible to see that 100% of both KIF2 (panel A3) or KIF2β-positive vesicles (panel B3) are positive for lamp-1 but some lamp-positive lysosomes are not labeled with the myc antibody (green vesicles in Figure 7A, A3 and B3).

To confirm the lysosomal localization of the KIF2-like isoforms and exclude that it may be an artifact of overexpression, double labeling was performed using anti-KIF2 antiserum and anti-lamp-1 monoclonal antibody in saponin-extracted, non-transfected fibroblasts. This clearly showed that 70–80% of lamp-1-labeled tubulo-vesicular lysosomes were simultaneously immunopositive for KIF2/2β (data not shown; however, see Figure 9B), indicating that the lysosomal association of the motor proteins is bona fide.

### *Overexpression of KIF2 and KIF2β causes aberrant lysosomal morphology and peripheral dispersion*

In addition to having identified lysosomes as the cytosolic compartment with which KIF2/2β is associated, we observed that KIF2β-immunopositive lysosomes were strikingly larger and less numerous in transfected cells than in non-transfected cells (0.25–1.5 μm and occasionally up to 3 μm in size in transfected cells compared with 0.25 μm on average in non-transfected cells; compare Figures 5b and 7a with Figure 7b). Furthermore, whereas normal lysosomes in non-transfected cells occupied a characteristic perinuclear rim-like position (Figure 7b, A1 and A2), KIF2β-labeled lysosomes of transfected cells were dispersed throughout the cytoplasm and were usually localized peripherally, at some distance from the nucleus and some were close to the plasma membrane (Figures 6 and 7a). A statistical analysis of lysosome positioning in transfected versus non-transfected cells showed that the closest distance of enlarged lysosomes to the edge of the

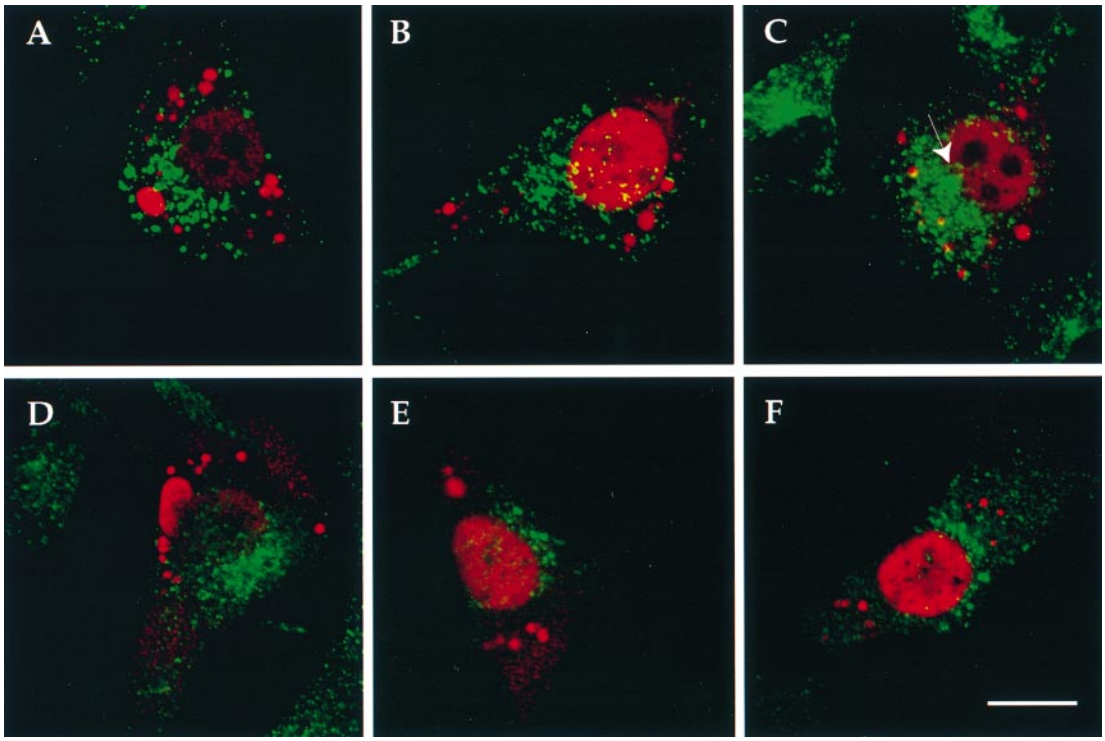


**Fig. 6.** Double immunolocalization of myc-tagged KIF2 or 2β (red) and various markers of the endocytic pathway (green) in transiently transfected NIH 3T3 mouse fibroblasts shows no co-localization. (**A**) Anti-mycKIF2 and anti-eea1, a marker for early endosomes; (**B**) anti-mycKIF2 and FITC-labeled transferrin, internalized for 5 min as described in Materials and methods, as a marker for the early endocytic pathway; (**C**) anti-mycKIF2β and FITC-labeled transferrin internalized for 20 min to label both early endosomes and the recycling compartment [in this example the perinuclear recycling compartment is visible (arrow)]; (**D**) anti-mycKIF2 and anti-transferrin receptor, also a marker for early and recycling endosomes; (**E**) anti-mycKIF2 and anti-mpr1, an antibody recognizing the cytoplasmic tail of the mannose-6-phosphate receptor (CI-MPR), serving as a marker for late endosomes; (**F**) anti-mycKIF2 and anti-mpr2, an antibody recognizing the lumenal domain CI-MPR. Scale bar in confocal micrographs: 8.5 μm.

nucleus was 1.77 ± 0.56 μm (average ± SD) and the furthest distance 11.65 ± 3.43 μm. The respective values for non-transfected cells were 0 and 7.72 ± 2.38 μm, clearly showing that not only were enlarged lysosomes more dispersed throughout the cytoplasm but overall were positioned more remotely from the nucleus.

To analyze the association of KIF2β with lysosomes and demonstrate that the motor protein is membrane-bound, we examined the effect of mild extraction with the detergents saponin and Triton X-100 in transfected cells, before fixation. The use of detergent prior to fixation results in the removal of non-membrane-bound cytosolic protein. Saponin at 0.01% and Triton X-100 at 0.25% were tested for different incubation periods, ranging from 20 s to 2 min, applied prior to cell fixation and immunofluorescence processing. Brief pre-extractions (40 s for saponin and 30 s for Triton X-100) did not seem to have any effect on either KIF2β distribution (as illustrated by myc-labeling, Figure 8, A1 and A2) or lamp-1 staining of lysosomes (Figure 8, B1 and B2). Under these relatively mild pre-extraction conditions, lysosomal membrane proteins and associated proteins appear to remain intact (see also inset in Figure 8, C1). An interesting observation was that brief pre-extraction, especially with saponin, revealed a distinct labeling of what appeared as a characteristic microtubule network (Figure 8, A1, A2 and A2 inset at higher magnification), which had not previously been detectable under standard immunofluorescent processing of transfected cells. Both myc-KIF2β and lamp-1 remained non-pre-extractable, even at longer incubations with saponin (2 min, Figure 8, B1 and B2), although the 'MT-staining' was no longer detectable or was greatly reduced. Nevertheless, more prolonged Triton X-100 pre-extraction (2 min) clearly abolished all lamp-1 and myc labeling (Figure 8, D1 and D2), strongly suggesting that under these conditions, membrane association of both resident lysosomal proteins and interacting proteins is disrupted.

Finally, immunolocalization was also performed on thawed cryosections of fixed, non-transfected, NIH 3T3 cells using electron microscopy (EM). In single-labeling experiments KIF2β decoration was observed close to vesicular structures that resembled lysosomes and were clearly distinct from ER membranes, Golgi stacks or clathrin-coated vesicles (Figure 9A) but also internally located in structures that had the appearance of caveolae and were decorated with caveolin antibodies (data not shown). Importantly, and consistent with our observation in immunofluorescence studies of KIF2 or 2β-transfected fibroblasts, EM double-immunolabeling experiments with non-transfected cells revealed that KIF2β decoration co-localized in structures that were heavily labeled for lamp-1. Figure 9B gives a clear example of simultaneous decoration of lysosomal membranes with secondary antibodies conjugated with different size gold particles: 5 nm, indicative of lamp-1 immunoreactivity, and 10 nm, indicative of KIF2β.

## Discussion

In the present work we report the identification of a new member of the KIFs, KIF2β. This is an alternatively

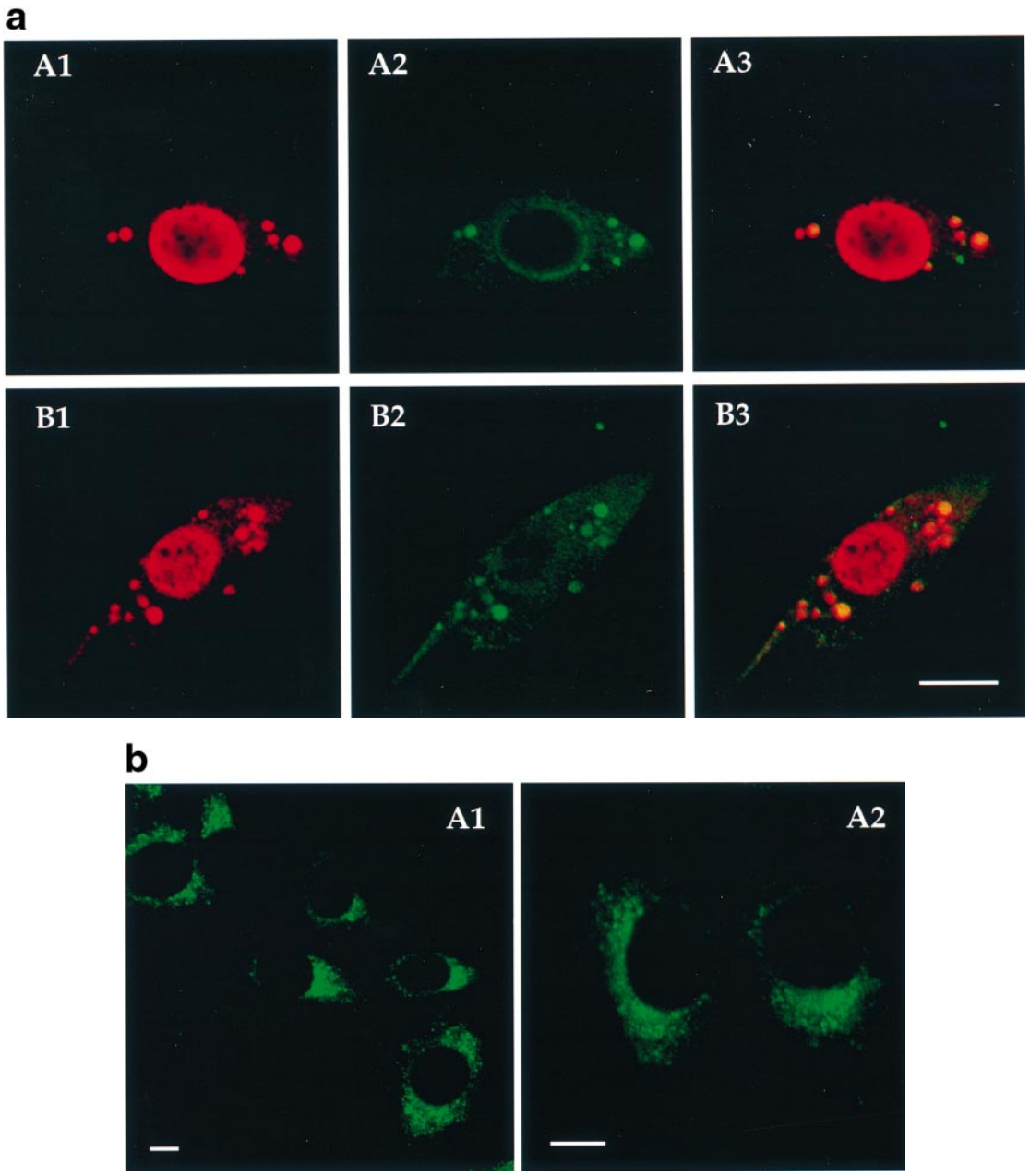


**Fig. 7.** (**a**) Identification of lysosomes as the site of cytoplasmic localization of KIF2 or 2β shown by co-localization of KIF2 or 2β and lamp-1 in transiently transfected mouse NIH 3T3 fibroblasts. (A1 and B1) Anti-mycKIF2 and anti-myc-KIF2β staining, respectively; (A2 and B2) anti-lamp-1, a marker of lysosomes in fibroblasts; (C1 and C2) overlay, revealing cytoplasmic co-localization. Exactly the same results were obtained with myc-KIF2 or 2β-transfected cells and an anti-lamp-2 antibody. Scale bar in confocal micrographs: 8 μm. (**b**) lamp-1-staining in non-transfected NIH 3T3 to illustrate the normal morphology and positioning of the lysosomal compartment as a dense perinuclear rim. (A1) Wide field with six cells; (A2) detail of two cells at higher magnification. Scale bars in confocal micrographs: 5 μm.

spliced variant isoform of the known KIF2 protein (Noda *et al.*, 1995). Besides differences in sequence, KIF2β is distinct from KIF2 in (i) the pattern of developmental regulation, and (ii) the type of expressing cells. KIF2 and KIF2β are expressed at similar levels in early embryonic hippocampal tissue but at later developmental stages KIF2 is the main (or sole) isoform of mature hippocampal neurons and it becomes undetectable in glial cells (Figure 3A). Conversely, our RT–PCR and Western blot analysis shows KIF2β as the only isoform in astrocytes and also in fibroblasts. Although the presence of KIF2β in early embryonic hippocampus mRNA could be attributed exclusively to mRNA from cells of non-neuronal origin (glia), it is also plausible that KIF2β expression at this stage may originate from neuronal precursors or even from early differentiating neurons. *In situ* hybridization in neurons using a KIF2β-specific probe could resolve this point, however it is not possible to design such probes as there are no KIF2β-unique sequences that would discriminate KIF2β from KIF2. In conclusion, our analysis demonstrates that, upon differentiation, KIF2 is exclusively neuronal and KIF2β is exclusively or predominantly non-neuronal.

Our most interesting finding was the identification of

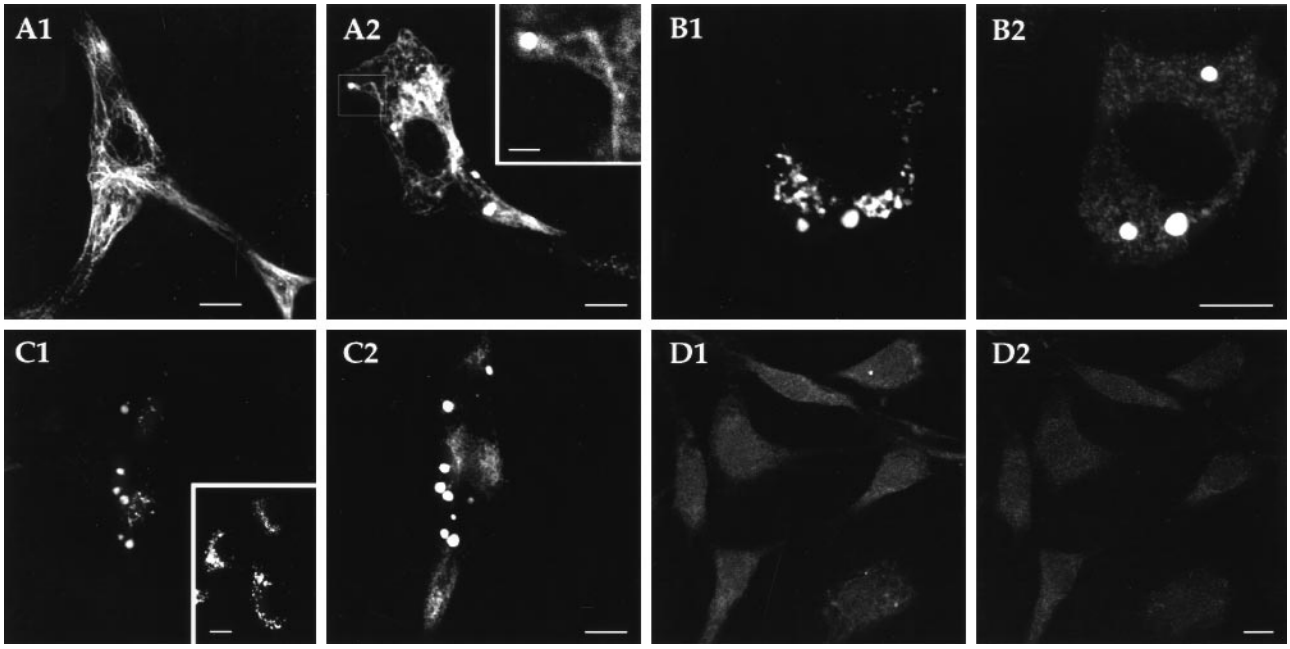


**Fig. 8.** Effect of detergent extraction, prior to fixation, on lysosomal association of KIF2β in transfected NIH 3T3. Top panels show cells pre-extracted with 0.01% saponin (A1 and A2 for 40 s; B1 and B2 for 2 min) and the bottom panels cells pre-extracted with 0.25% Triton X-100 (C1 and C2 for 30 s; D1 and D2 for 2 min). (A1 and A2) Characteristic examples of myc-immunoreactivity in transfected cells that were subjected to brief saponin pre-extraction reveal distinct labeling of what appears like MT as well as lysosomes. Note the localization of myc-labeled lysosomes on such 'MT-tracks' (inset in A2 for detail at higher magnification). (B1 and B2) Even at more prolonged saponin pre-extraction, both lamp-1- (B1) and myc-KIF2β- (B2) association with lysosomal membranes is maintained (but MT-labeling is no longer visible). (C1 and C2) A similar immunofluorescent pattern as with saponin pre-extraction is obtained at short Triton X-100 pre-extraction (although the MT staining is much harder to discern and record; C1 for lamp-1 and C2 for myc). Inset in (C1) illustrates typical, perinuclear, dense lamp-1 labeling in three untransfected cells on the same coverslip, to indicate that this brief extraction appears not to have any effect on lamp association with lysosomal membranes. (D1 and D2) Both antigens are extractable at longer Triton X-100 pre-extraction periods (D1 for lamp-1 and D2 for myc). A large, representative field including seven cells is shown, devoid of leveling for both antigens. Scale bars in confocal micrographs: 10 μm for all panels, 2.5 μm for the insets.

lysosomes as the cytoplasmic vesicles with which KIF2β associates. Both EM localization in non-transfected fibroblasts and light microscopy results in transfected cells make us confident that lysosomes are the native *in vivo* site with which KIF2β is functionally related. We carried out a series of control experiments illustrating that our anti-tag antibody was a reliable marker for following the fate of transiently overexpressed protein, that our transfection vector was a reliable tool for the expression and appropriate targeting of proteins with diverse and distinct intracellular localizations, and that the localization of expressed proteins was consistent and irrespective of the tag used. More importantly, we showed that over-expression of other kinesin superfamily proteins in NIH 3T3 cells, under identical conditions, resulted in appropriate localization in each case. Finally, consistent with a role of a lysosome plus-end transporter for KIF2β, the staining of lysosomes was membrane-associated, both on the basis of visualization on thin confocal optical sections (Figure 5b, G), detergent pre-extraction (Figure 8) and also by EM (Figure 9). The presence of KIF2β in caveolae-like structures in non-transfected cells, which was observed by EM, may suggest a possible trafficking pathway between caveolae and lysosomes, but this point has to be investigated further before conclusions can be drawn.

In our transient transfection assays as well as by immunofluorescence using polyclonal anti-KIF2, we also identified in interphase fibroblasts, but not in neurons, the nucleus as a site of distinct association of KIF2β. This is an interesting finding in the light of the identification of KIF2 as the only (or major) isoform in terminally differentiated, post-mitotic neurons and of KIF2β as the isoform expressed in cells which maintain their mitotic activity. While it may be tempting to speculate that KIF2 has a unique role in cytoplasmic transport in non-mitotic cells whereas KIF2β, in addition to this role, may have an additional role during mitotic division in proliferating cells, we have, nevertheless, not been able to observe tagged-protein accumulation at the poles of the mitotic spindle, contrary to labeling of these structures with anti-KIF2 monoclonal antibody in untransfected mitotic fibroblasts. The reason for this discrepancy is not clear, but a possible explanation could be that spindle labeling by the anti-KIF2 monoclonal antibody may be due to crossreactivity to mouse CAK/KCM1, the murine homologue of hamster mitotic kinesin-like protein MCAK (Wordeman and Mitchison, 1995) which has >70% sequence similarity to KIF2.

Overexpression of KIF2 or KIF2β in fibroblasts resulted in complete re-organization of the lysosomal compartment in transfected cells. KIF2β-associated lysosomes were (i) strikingly larger and less numerous than their counterparts in non-transfected cells (up to 5–10 times larger, compare Figure 7a with b); and (ii) they were clearly not confined to the juxtanuclear sites, typical of non-transfected cells, but were dispersed throughout the cytoplasm, nearer the plasma membrane and at a distance from the nucleus (again compare Figures 7a with b). For several reasons, this peripheral location upon overexpression is not surprising. First, because KIF2/2β are conven-

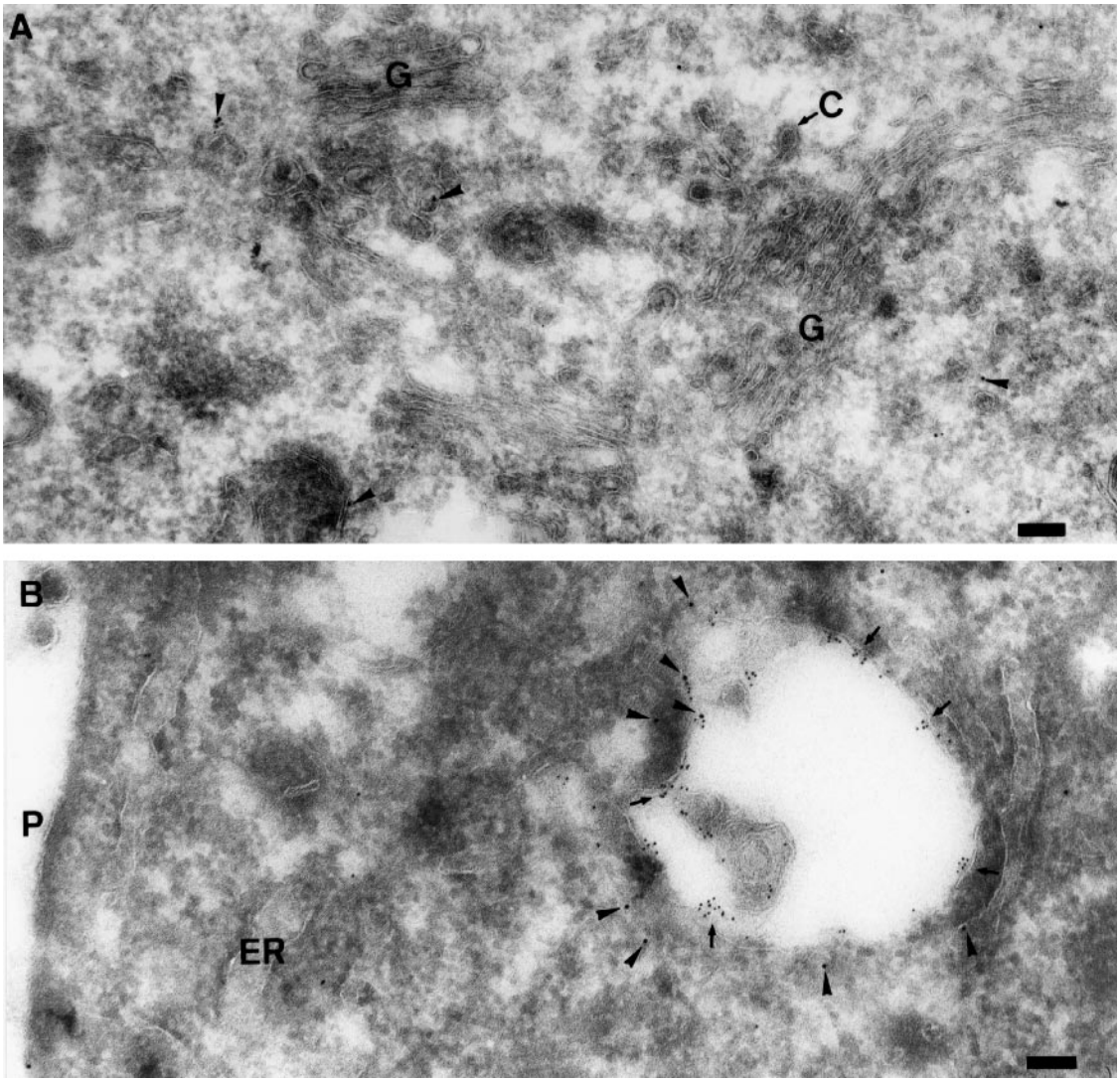


**Fig. 9.** Electron microscopy immunolocalization of KIF2β in mouse NIH 3T3 fibroblasts. (**A**) KIF2β single labeling. Gold particles (arrowheads) are mainly found in the proximity of tubular and vesicular membranous organelles. Unlabeled Golgi cisternae (G) and clathrin-coated vesicles (C, arrow) are indicated to emphasize the specificity of the labeling. (**B**) KIF2β (10 nm gold particles; arrowheads) and lamp-1 (5 nm gold particles; arrows) double labeling co-localizes on the periphery of a lysosome. Note the absence of labeling for either marker over other membranes, like the endoplasmic reticulum (ER) or the plasma membrane (P). Scale bars in electron micrographs: 100 nm.

tional plus-end-directed motors and MT plus-ends of vertebrate cells in culture face the cell periphery. Secondly, strong evidence about the possible implication of a kinesin-like protein in centrifugal lysosome translocation has accumulated in the last 10 years (see Introduction), although the identity of the specific, endogenous kinesin-like protein had remained elusive. We propose that KIF2β in non-neuronal cells is an endogenous plus-end-directed motor that moves lysosomes from their usual site of cytoplasmic accumulation near the nucleus to more peripheral sites close to the plasma membrane.

Lysosomes are highly dynamic organelles and have the ability of homotypic fusion as well as fusion with endosomes (Ferries *et al.*, 1987; Deng and Storrie, 1988; Storrie and Desjardins, 1996, Ward *et al.*, 1997). It remains to be elucidated whether the large, KIF2β-associated, peripherally located lysosomes are formed as a result of enhanced clustering and/or fusion or inhibition of fission due to increased motor protein activity. It also remains to be tested whether these lysosomes are functionally active (i.e. by measuring concentration of endocytosed ligands). Preliminary experiments (not shown) suggest that they are not active and upon internalization for up to 2 h with lucifer yellow, a fluid-phase marker, we could not detect ligand in these large lysosomes, suggesting that KIF2β overexpression induces a type of response not compatible with ligand degradation. However, endocytosis *per se* is not perturbed in the large lysosome-bearing cells, as Tf was internalized normally into early endosomes and the recycling compartment (Figure 6B and C).

Our work shows that KIF2β is a motor protein that associates with lysosomes in non-neuronal cells. Moreover, our results suggest that KIF2β overexpression may be responsible for changing the balance between two opposing forces that keep lysosomes in their juxtanuclear position, of dynein, the minus-end-directed motor attracting lysosomes close to MT minus-ends and of the kinesin-like, plus-end-directed motor, capable of translocating them in the opposite direction, resulting in net lysosome movement towards the cell periphery. Such

'imbalance' in favor of KIF2β may normally be triggered as part of certain physiological responses, such as, for example, the centrifugal transportation of lysosomes and their recruitment to the plasma membrane site of parasite invasion during *Trypanosoma cruzi* infection (Tardieux *et al.*, 1992; reviewed by Andrews, 1995). *Trypanosoma cruzi* infection (otherwise known as Chagas' disease) is a serious, potentially lethal and incurable health hazard putting at risk 25% of the total South and Central American population and causing chronic ailments in about 16% of affected individuals (World Health Organisation data on Chagas' Disease Control, Internet site: www.who.ch). Given that we propose KIF2β as a motor protein involved in lysosomal outward movement, it is attractive to envisage that its expression and/or its recruitment from cytoplasmic pools may be induced by the parasite, ultimately facilitating lysosome-mediated parasite entry. It appears tempting to test whether blocking KIF2β expression in host cells may inhibit parasite entry without affecting host cell viability. If this occurs, then KIF2β antisense oligonucleotides could act as preventive agents for parasite infection.

## Materials and methods

### *Hippocampal mouse cell cultures, mouse astrocyte cultures and NIH 3T3 cell line*

Primary cultures of hippocampal neurons were prepared from isolated hippocampi of E15 mouse embryos, according to the protocol of Goslin and Banker (1991) at densities of $1–4\times10^5$ cells per 60 mm diameter dish. To reduce glial proliferation, the DNA synthesis inhibitor cytosine b-D-arabinofuranoside was added to the cultures at 5 μM, 5 days after plating. Cells were cultured for periods of between 1 day and 2 weeks in $N_2$ MEM (Bottenstein and Sato, 1979) at 37°C in 5% $CO_2$ and harvested for poly(A)$^+$ RNA purification or for immunofluorescence at distinct neuronal developmental stages [stages 1–5 according to Dotti *et al.* (1988)].

Proliferating pure astrocyte cultures [prepared according to Levison and McCarthy (1991)] were derived from newborn animals and maintained in MEM medium, containing 10% horse serum, 0.6% glucose, 2 mM glutamine and 1 ng/ml fibroblast growth factor.

NIH 3T3 mouse fibroblasts were cultured in DMEM containing 10% fetal calf serum (FCS; Gibco-BRL), 2 mM glutamine, 50 U/ml penicillin/streptomycin and maintained at 37°C in 5% $CO_2$.

### *Antibodies*

The following primary antibodies were used for immunolabeling: anti-myc epitope, affinity purified, mouse monoclonal antibody 9E10 (Evan *et al.*, 1985; maintained by A.Sawyer at the EMBL; 1:800 dilution for immunofluorescence, IF), anti-myc epitope, affinity-purified rabbit antiserum (Röttger *et al.*, 1998; a gift from T.Nilsson, EMBL; 1:50 for IF), anti-lamp-1 rat monoclonal antibody 1D4B (lysosome-associated membrane protein 1) and anti-lamp-2 rat monoclonal antibody ABL-93 (originally developed by T.August and obtained from Developmental Studies Hybridoma Bank, University of Iowa, USA; 1:100 for IF, and EM), anti-mpr1 and anti-mpr2 rabbit antisera to the cytoplasmic tail or the lumenal domain, respectively, of the cation-independent mannose-6-phosphate receptor (Griffiths *et al.*, 1988; provided by J.Lanoix, EMBL; 1:100 for mpr1 and 1:150 for mpr2 for IF), anti-eea1 (early endosomal antigen) human autoimmune antiserum (Mu *et al.*, 1995; a gift of H.Stenmark, EMBL; 1:1000 for IF), anti-transferrin rabbit antiserum (Zymed, Germany; 1:50 for IF), anti-transferrin receptor, mouse monoclonal antibody H68.4 (Zymed; 1:50 for IF) and affinity-purified rabbit antiserum to KIF2 (Noda *et al.*, 1995; 1:100 for IF and Western blotting, and 1:10 for EM).

The secondary antibodies used were: fluorescein isothiocyanate (FITC)-conjugated, goat anti-mouse IgG1 (Southern Biotechnology Associates, Birmingham, AL, USA), FITC-conjugated, donkey anti-mouse IgG (Dianova, Hamburg, Germany), Texas Red-conjugated, goat anti-mouse IgG+M (Dianova), rhodamine (TRITC)-conjugated, donkey anti-mouse IgG+M (Dianova), FITC-conjugated, donkey anti rabbit IgG (Dianova), TRITC-conjugated, donkey anti-rabbit IgG (Dianova), FITC-conjugated, goat anti-rat IgG (Cappel, Organon Teknika Corporation, Durham, NC, USA) and TRITC-conjugated donkey anti-human Ig (Dianova).

### *Oligonucleotides*

The following pairs of oligonucleotides were used for this work:
Set 1: (upstream) actgtggcagctgttaagaa, (downstream) aatccaagctccct-ctgaagtc. This set was designed to amplify an internal region, included between nucleotides 709 and 1048, of the ORF of KIF2 (EMBL D12644). Set 2: (upstream) gactgcagactgccgaatacac, (downstream) ccgctcgagttag-tagcaaacgccaactta. This set was designed to amplify sequences containing the full-length ORF of KIF2 (nucleotides 478–2673) for direct ligation into the T/A cloning vector (InVitrogen, The Netherlands) and subsequent nucleotide sequencing. Set 3: (upstream) cgggatccgcaatggtaacatctttaaatg, (downstream) ccgctcgagttagtagcaaacgccaactta. This set was designed to amplify the full-length ORF of KIF2 (nucleotides 502–2673 ) and enable its cloning into tagged mammalian expression vectors. The upstream oligo contains an additional 5′ *Bam*HI site and the downstream oligo a 5′ *Xho*I site, engineered to enable cloning and maintenance of the correct reading frame upon subsequent ligation of the *Bam*HI–*Xho*I digested PCR products into the mammalian expression vectors pSVmyc1.0 and pSVhis1.0 (see below). Set 4: (upstream) ggatcgatttgcitayggrcaracngg, (downstream) agtagcaaacgccaacttaga. To amplify another internal region of the OFR of KIF2 (nucleotides 1288–2671). The upstream oligo is degenerate and bears an additional 5′ *Cla*I site. Set 5: (upstream) tgggaagctggtcatcaatgggaaacc, (downstream) tcatggatgaccttggccagggg. To amplify part of the ORF (nucleotides 233–538) of the mouse glyceraldehyde-3-phosphate dehydrogenase cDNA (mGAPDH; EMBL M32599), used as an internal control for PCR amplification.

### *RNA extraction and RT–PCR*

Poly(A)$^+$ RNA was directly affinity-purified from staged hippocampal cultures (typically starting from $2\times10^6$ cells), from isolated hippocampi (2–4 organs) of E13, E15, juvenile (2.5 weeks), or adult (3-month-old) mice, from pure mouse astrocyte cultures and NIH 3T3 mouse fibroblast cultures, using the QuickPrep Micro mRNA purification kit (Pharmacia Biotech, Sweden). cDNA was synthesized with MMLV reverse transcriptase from equivalent amounts of poly(A)$^+$ RNA from each source (typically 10 ng), using the Advantage RT-for-PCR kit (Clontech Laboratories, Inc. Palo Alto, CA, USA).

PCRs were carried out using the Expand Long Template PCR system (Boehringer Mannheim, Germany) on a Perkin-Elmer model gene Amp PCR system 2400. The full-length ORF of KIF2 and KIF2β was amplified with oligo set 2 or 3 (Figure 1B), using the following protocol: 2 min denaturation of the E15 cDNA template at 94°C; 33 cycles of a 10 s denaturation at 94°C; a 30 s annealing at 55°C; and an extension of 3 min at 68°C; followed by a final 5 min extension at 68°C. The same protocol, but with 30 cycles, was used for the study of the developmental pattern of expression of KIF2 and 2β during neuronal differentiation *in vivo* and *in vitro* (Figure 3), using oligo set 4 for the simultaneous amplification of the two isoforms and oligo set 5 as an internal control. Finally, for the diagnostic PCR co-amplification of KIF2 and 2β with oligo set 1 (Figure 1A), the extension time was reduced to 1 min.

PCR products were directly cloned into vector pCR2.1, using the Original T/A cloning kit (InVitrogen) and sequenced on both strands by the EMBL sequencing service with cycle sequencing and internal labeling on a robotic workstation.

### *Standard molecular biology techniques and Western blotting*

All standard molecular biology techniques (plasmid purifications, restriction digests, ligations, blue/white bacterial colony selection, etc) were performed according to Sambrook *et al.* (1989). SDS–PAGE electrophoresis was carried out on 7% gels as described by Laemmli (1970) and Western blotting was performed on a mini trans blot wet transfer blotting apparatus (Bio-Rad) and developed with the enhanced chemiluminescence kit (Amersham Life Sciences). SDS–PAGE samples were prepared by direct lysis of culture monolayers or tissue homogenization in 50 mM Tris pH 8.0, containing 1% SDS and a cocktail of protease inhibitors, followed by standard TCA precipitation.

### *Construction of mammalian transfection vectors*

A modified version of mammalian expression vector pSG5 (Stratagene, Germany), with an extended polylinker cloning site, was used to construct the tagged expression vectors pSVmyc 1.0 and pSVhis 1.0. For pSVmyc 1.0, an oligonucleotide linker, encoding part of the human c-myc epitope (AS**KLISEEDL**GS), was inserted in-frame to the initiator Methionine and an in-frame $(catcac)_3$ sequence, corresponding to a poly-histidine track ($His_6$) was present in pSVhis1.0. The complete ORFs of KIF2 and KIF2β were ligated into pSVmyc1.0/his 1.0 as *Bam*HI–*Xho*I in-frame inserts, generating 5′-myc or his-tagged versions of the two kinesin

isoforms (pSVmycKIF2, pSVmycKIF2β, pSVhisKIF2 and pSVhis-KIF2β). The integrity of the coding sequences of all plasmids was confirmed by full-length nucleotide sequencing.

Plasmid pSVmycL22, bearing a 5′ myc-tagged version of the human ribosomal protein L22 (Toczyski *et al.*, 1994), was constructed by in-frame ligation of the PCR-amplified ORF of L22 and used as positive control for transient transfections, together with a plasmid encoding a myc-tagged XKLP1 kinesin of *Xenopus* (Vernos *et al.*, 1995) (a gift from Isabelle Vernos, EMBL) and pSVmyc1.0, as a negative control.

#### *Transient transfections of myc-tagged KIF2 in hippocampal neurons and NIH 3T3 cell line*

E18 rat embryonic hippocampal cultures, growing on coverslips in 60 mm dishes, were transfected 24 h after plating. Prior to addition to the cultures, 10 μg of pSVmKIF2 in 250 mM $CaCl_2$ were mixed with an equal volume of 2× HBS (274 mM NaCl, 10 mM KCl, 1.4 mM $Na_2HPO_4$, 15 mM glucose, 42 mM HEPES pH 7.07) and a calcium/phosphate precipitate was allowed to form for 30 min at room temperature. Three hundred and sixty microlitres of the transfection mix was added to each dish for 20 min at 37°C in 5% $CO_2$ and the transfection was stopped by washes with $N_2$ MEM. Cultures were subsequently maintained at 37°C in 5% $CO_2$ and coverslips were sampled and processed for immunofluorescence 3 days post-transfection.

Exponentially growing NIH 3T3 cultures were harvested and replated onto coverslips in 60 mm diameter dishes, 24 h prior to transfection. Routinely, 1–5 μg of plasmid were added to 250 mM $CaCl_2$, mixed with an equal volume of 2× BES-buffered saline (50 mM N,N-bis [2-hydroxyethyl]-2-aminomethanesulfonic acid, 280 mM NaCl and 1.5 mM $Na_2HPO_4o2H_2O$, pH 6.96), incubated for 15 min at room temperature and added dropwise, in a total volume of 400 μl, to each dish of cells in complete DMEM. Transfections were allowed to proceed for 20 h at 37°C in 5% $CO_2$, the transfection medium was then removed, and the dishes rinsed three times with fresh DMEM and incubated under standard conditions. Coverslips were retrieved for immunofluorescence 12–36 h after removal of the transfection medium.

#### *Immunolabeling of cultured cells and transferrin internalization*

Cells grown on glass coverslips were fixed with 3.7% paraformaldehyde in PHEM buffer (65 mM PIPES, 30 mM HEPES pH 6.9, 10 mM EGTA and 2 mM $MgCl_2$) for 10 min. They were quenched with 50 mM ammonium chloride in PBS for 10 min, permeabilized for 10 min with 0.5% Triton X-100 in PHEM buffer and blocked with 2% BSA, 2% FCS, 0.2% fish skin gelatin ('blocking mix') in PBS for 30 min. Cells were incubated with primary antibodies, in PBS containing 5% blocking mix, for 1 h at room temperature. For double labeling, incubation was carried out sequentially for each of the primary antibodies and secondary antibodies were applied as a mixture. For double immunofluorescence using anti-myc mouse monoclonal and anti-lamp-1 or 2 rat monoclonal antibodies, the mouse primary and anti-mouse secondary antibodies were sequentially applied first, followed by sequential incubations with the rat primary and anti-rat secondary antibody. Coverslips were mounted with Mowiol (Merck, Germany), containing 100 mg/ml DABCO (Sigma, Germany) as an anti-fading agent.

For detergent pre-extractions of transfected cells prior to immunolabeling, coverslips were quickly rinsed in PBS, equilibrated in PHEM for 1 min and subsequently dipped in either 0.01% saponin in PHEM or 0.25% Triton X-100 in PHEM for times ranging between 20 s and 2 min, at room temperature. Cells were then immediately fixed and processed for immunofluorescence as described above but without further permeabilization.

*In vivo* labeling of the endocytic pathway with transferrin in NIH 3T3 cells was performed according to Hémar *et al.* (1997). Briefly, cultures were depleted of transferrin with a 2 h incubation in FCS-free DMEM and then allowed to internalize FITC-tranferrin at a final concentration of 50 μg/ml in DMEM, between 10–30 min at 37°C in 5% $CO_2$. Coverslips were rinsed at different time points with cold PBS and then immediately fixed and processed for immunofluorescence as described above, except that permeabilization was carried out for 5 min with 0.25% Triton X-100 in PHEM buffer.

#### *Epifluorescence, confocal and electron microscopy*

Immunofluorescent preparations were analyzed on a Zeiss Axiophot light microscope or on a Zeiss LSM510 model confocal microscope using excitation wavelengths of 488 nm (FITC-coupled antibodies) or 543 nm (TRITC and Texas Red). Confocal images were recorded and then examined and printed using Adobe Photoshop 4.0 and Adobe Illustrator 6.0. Three-dimensional reconstruction imaging of stacks of serial confocal sections (Figure 5b, G) was performed using the software of the Zeiss LSM510. Precision measurements of distances of lysosomal structures from the nucleus were carried out in batches of 25 transfected or non-transfected cells on the same coverslip, using the LSM software. Such statistical analysis was carried out several times in independent experiments and the results presented are from a representative sampling.

For EM, confluent monolayers of NIH 3T3 cells grown in 6 cm dishes, were fixed *in situ* by addition of 8% paraformaldehyde/0.2% glutaraldehyde in 2× PHEM to an equal volume of medium. Cells were scraped from the dish after a 2 h incubation at room temperature and collected by centrifugation. The first fixative was then replaced by 8% paraformaldehyde in PHEM and left overnight at 4°C. Cells were washed with 0.12% glycine in PBS, resuspended in PBS containing 2% low melting agarose at 37°C, spun for 5 min at 13 000 *g* and immediately put on ice. The agarose-embedded cells were cut in small blocks, infiltrated with 2.3 M sucrose and frozen in liquid nitrogen. Cryosections were singly or doubly labeled with appropriate combinations of primary and 5 or 10 nm gold-labeled secondary antibodies (Dianova), according to Slot *et al.* (1991), and examined with a Zeiss EM10.

## Acknowledgements

We would like to thank the EMBL DNA sequencing and oligonucleotide services and Doros Panayi at the photolab for excellent photographic assistance. We are indebted to Reiner Saffrich for carrying out nuclear microinjections of NIH 3T3 cells. We are very grateful to Emilio Rubino for dedicated technical assistance, to Bianca Hellias for her help and expert maintenance of neuronal cultures and to Sybille Schleich for help with electron microscopy. We are also grateful to Drs Marino Zerial, Tommy Nilsson, Joel Lanoix, Harald Stenmark and Alan Sawyer, all at the EMBL, for kindly providing antibodies, to Dr Carol Murphy (EMBL/University of Ioannina, Greece) for her gift of FITC-transferrin and to Dr Isabelle Vernos at the EMBL for her gift of myc-XKLP1 plasmid. N.S. was a recipient of a Human Capital and Mobility Fellowship from the European Union and a short-term Fellowship from FEBS. C.G.D. is partially funded by the Deutsche Forschungsgemeinschaft (DFG, grant SFB 317).

## References

Aizawa,H., Sekine,Y., Takemura,R., Zhang,Z., Nangaku,M. and Hirokawa,N. (1992) Kinesin family in murine central nervous system. *J. Cell Biol.*, **119**, 1287–1296.

Andrews,N.W. (1995) Microbial subversion of phagocytosis: lysosome recruitment during host cell invasion by *Trypanosoma cruzi. Trends Cell Biol.*, **5**, 133–137.

Aniento,F., Emans,N., Grifiths,G. and Gruenberg,J. (1993) Cytoplasmic dynein-dependent vesicular transport from early to late endosomes. *J. Cell Biol.*, **123**, 1373–1387.

Bloom,G. and Endow,S. (1994) Motor proteins. 1: kinesins. *Protein Profile*, **1**, 1059–1116.

Bloom,G. and Endow,S. (1995) Motor proteins. 1: kinesins. *Protein Profile*, **2**, 1105–1171.

Bottenstein,J.E. and Sato,G.H. (1979) Growth of a rat neuroblastoma cell line in serum-free supplemented medium. *Proc. Natl Acad. Sci. USA*, **76**, 514–517.

Burkhardt,J.K., Echeverri,C.J., Nilsson,T. and Vallee,R.B. (1997) Overexpression of the dynamitin (p50) subunit of the dynactin complex disrupts dynein-dependent maintenance of membrane organelle distribution. *J. Cell Biol.*, **139**, 469–484.

Chelsky,D., Ralph,R. and Lonak,G. (1989) Sequence requirements for synthetic peptide-mediated translocation to the nucleus. *Mol. Cell. Biol.*, **9**, 2487–2492.

Debernardi,S., Fontanella,E., De Gregorio,L., Pierotti,M.A. and Delia,D. (1997) Identification of a novel human kinesin-related gene (HK2) by the cDNA differential display technique. *Genomics*, **42**, 67–73.

Deng,Y. and Storrie,B. (1988) Animal cell late lysosomes rapidly exchange membrane proteins. *Proc. Natl Acad. Sci. USA*, **85**, 3860–3864.

Dillman,J.F., Dabney,L.P. and Pfister,K.K. (1996) Cytoplasmic dynein is associated with slow axonal transport. *Proc. Natl Acad. Sci. USA*, **93**, 141–144.

Dotti,C.G., Sullivan,C.A. and Banker,G.A. (1988) The establishment of polarity by hippocampal neurons in culture. *J. Neurosci.*, **8**, 1454–1468.

Evan,G.I., Lewis,G.K., Ramsay,G. and Bishop,M.J. (1985) Isolation of monoclonal antibodies specific for human c-*myc* proto-oncogene product. *Mol. Cell. Biol.*, **5**, 3610–3616.

Feiguin,F., Ferreira,A., Kosik,K.S. and Caceres,A. (1994) Kinesin-mediated organelle translocation revealed by specific cellular manipulations. *J. Cell Biol.*, **127**, 1021–1039.

Ferries,A.L., Brown,J.C., Park,R.D. and Storrie,B. (1987) Chinese hamster ovary cell lysosomes rapidly exchange contents. *J. Cell Biol.*, **105**, 2703–2712.

Geuze,H.J., Stoorvogel,W., Strous,G.J., Slot,J.W., Bleekemolen,J.E. and Mellman,I. (1988) Sorting of mannose 6-phosphate receptors and lysosomal membrane proteins in endocytic vesicles. *J. Cell Biol.*, **107**, 2491–2501.

Goslin,K. and Banker,G. (1991) Rat hippocampal neurons in low density culture. In Banker,G. and Goslin,K. (eds), *Culturing Nerve Cells*. MIT Press, Cambridge, MA, USA, pp. 251–281.

Griffiths,G., Hoflack,B., Simons,K., Mellman,I. and Kornfeld,S. (1988) The mannose 6-phosphate receptor and the biogenesis of lysosomes. *Cell*, **52**, 329–341.

Harada,A., Takei,Y., Kanai,Y., Tanaka,Y., Nonaka,S. and Hirokawa,N. (1998) Golgi vesiculation and lysosome dispersion in cells lacking cytoplasmic dynein. *J. Cell Biol.*, **141**, 51–59.

Hémar,A., Olivo,J-C., Williamson,E., Saffrich,R. and Dotti,C.G. (1997) Dendroaxonal transcytosis of transferrin in cultured hippocampal and sympathetic neurons. *J. Neurosci.*, **17**, 9026–9034.

Herman,B. and Albertini,D.F. (1984) A time-lapse video image intensification analysis of cytoplasmic organelle movements during endosome translocation. *J. Cell Biol.*, **98**, 565–576.

Heuser,J. (1989) Changes in lysosome shape and distribution are correlated with changes in cytoplasmic pH. *J. Cell Biol*., **108**, 855–864.

Hirokawa,N. (1996a) Organelle transport along microtubules-the role of KIFs. *Trends Cell Biol.*, **6**, 135–141.

Hirokawa,N. (1996b) The molecular mechanism of organelle transport along microtubules: the identification and characterization of KIFs (kinesin superfamily proteins) *Cell Struct. Funct.*, **21**, 357–367.

Hirokawa,N. (1998) Kinesin and dynein superfamily proteins and the mechanism of organelle transport. *Science*, **279**, 519–526.

Hollenbeck,P.J. and Swanson,J.A. (1990) Radial extension of macrophage tubular late lysosomes supported by kinesin. *Nature*, **346**, 864–866.

Laemmli,U.K. (1970) Cleavage of structural proteins during the assembly of the head of bacteriophage T4. *Nature (Lond.)*, **227**, 680–685.

Levison,S.W. and McCarthy,K.D. (1991) Astroglia in culture. In Banker,G. and Goslin,K. (eds), *Culturing Nerve Cells*. MIT Press, Cambridge, MA, USA, pp. 251–281.

Lin,S.X.H. and Collins,C.A. (1992) Immunolocalization of cytoplasmic dynein to lysosomes in cultured cells. *J. Cell Sci.*, **101**, 125–137.

Mattaj,I.W. and Englmeier,L (1998) Nucleoplasmic transport: The soluble factor. *Annu. Rev. Biochem.*, **67**, 265–305.

Matteoni,R. and Kreis,T. (1987) Translocation and clustering of endosomes and lysosomes depend on microtubules. *J. Cell Biol.*, **105**, 1254–1265.

McGraw,T.E., Dunn,K.W. and Maxfield,F.R. (1993) Isolation of a temperature-sensitive variant Chinese hamster ovary cell line with a morphologically altered endocytic recycling compartment. *J. Cell Physiol*., **155**, 579–594.

Moore,J.D. and Endow,S.A. (1996) Kinesin proteins: a phylum of motors for microtubule-based motility. *BioEssays*, **18**, 207–219.

Morfini,G., Quiroga,S., Rosa,A., Kosik,K. and Cáceres,A. (1997) Suppression of KIF2 in PC12 cells alters the distribution of a growth cone nonsynaptic membrane receptor and inhibits neurite extension. *J. Cell Biol*., **138**, 657–669.

Mu,F.T. *et al*. (1995) EEA1, an early endosome-associated protein. EEA1 is a conserved alpha-helical peripheral membrane protein flanked by cysteine 'fingers' and contains a calmodulin-binding IQ motif. *J. Biol. Chem.*, **270**, 13503–13511.

Nakagawa,T., Tanaka,Y., Matsuoka,E., Kondo,S., Okada,Y., Noda,Y., Kanai,Y. and Hirokawa,N. (1997) Identification and classification of 16 new kinesin superfamily (KIF) proteins in mouse genome. *Proc. Natl Acad. Sci. USA*, **94**, 9654–9659.

Nakata,T. and Hirokawa,N. (1995) Point mutations of adenosine triphosphate-binding motif generated rigor kinesin that selectively blocks anterograde lysosome membrane transport. *J. Cell Biol*., **131**, 1039–1053.

Nangaku,M., Sato-Yoshitake,R., Okada,Y., Noda,Y., Takemura,R., Yamazaki.,H. and Hirokawa,N. (1994) KIF1B, a novel plus end-directed monomeric motor protein for transport of mitochondria. *Cell*, **79**, 1209–1220.

Noda,Y., Sato-Yoshitake,R., Kondo,S., Nangaku,M. and Hirokawa,N. (1995) KIF2 is a new microtubule-based anterograde motor that transports membranous organelles distinct from those carried by kinesin heavy chain or KIF3A/B. *J. Cell Biol*., **129**, 157–167.

Oda,H., Stockert,R.J., Collins,C., Wang,H., Novikoff,P.M., Satir,P. and Wolkoff,A.W. (1995) Interaction of the microtubule cytoskeleton with endocytic vesicles and cytoplasmic dynein in cultured rat hepatocytes. *J. Biol. Chem.*, **270**, 15242–15249.

Ogawa,K. and Mohri,H. (1996) A dynein motor superfamily. *Cell Struct. Funct.*, **21**, 343–349.

Okada,Y., Yamazaki,H., Sekine-Aizawa,Y. and Hirokawa,N. (1995) The neuron-specific kinesin superfamily protein KIF1A is a unique monomeric motor for anterograde axonal transport of synaptic vesicle precursors. *Cell*, **81**, 769–780.

Parton,R.G., Dotti,C.G., Bacallao,R., Kurtz,I., Simons,K. and Prydz,K. (1991) pH-induced microtubule-dependent redistribution of late endosomes in neuronal and epithelial cells. *J. Cell Biol.*, **113**, 261–274.

Rodriguez,A., Samoff,E., Rioult,M.G., Chung,A. and Andrews,N.W. (1996) Host cell invasion by trypanosomes requires lysosomes and microtubule/kinesin-mediated transport. *J. Cell Biol.*, **134**, 349–362.

Röttger,S. *et al.* (1998) Localization of three human polypeptide GalNAc-transferases in HeLa cells suggests initiation of O-linked glycosylation throughout the Golgi apparatus. *J. Cell Sci.*, **111**, 45–60.

Sambrook,J., Fritsch,E.F. and Maniatis,T. (1989) *Molecular Cloning: A Laboratory Manual.* Cold Spring Harbor Laboratory, Cold Spring Harbor, NY.

Scholey,J.M. (1996) Kinesin-II, a membrane traffic motor in axons, axonemes, and spindles. *J. Cell Biol.*, **133**, 1–4.

Sekine,Y., Okada,Y., Kondo,S., Aizawa,H., Takemura,R. and Hirokawa,N. (1994) A novel microtubule-based motor protein (KIF4) for organelle transports whose expression is regulated developmentally. *J. Cell Biol.*, **127**, 187–202.

Slot,J.W., Geuze,H.J., Gigengack,S., Lienhard,G.E. and James,D.E. (1991) Immunolocalisation of the insulin regulatable glucose transporter in brown adipose tissue in the rat. *J. Cell Biol.*, **113**, 123–135.

Sperry,A.O. and Zhao,L.P. (1996) Kinesin-related proteins in the mammalian testes: candidate motors for meiosis and morphogenesis. *Mol. Biol. Cell*, **7**, 289–305.

Storrie,B. and Desjardins,M. (1996) The biogenesis of lysosomes: is it a kiss and run, continuous fusion and fission process? *BioEssays*, **18**, 895–903.

Tardieux,I., Webster,P., Ravesloot,J., Boron,W., Lunn,J.A., Heuser,J.E. and Andrews,N. (1992) Lysosome recruitment and fusion are early events required for trypanosome invasion of mammalian cells. *Cell*, **71**, 1117–1130.

Toczyski,D.P., Matera,G.A., Ward,D.C. and Steitz,J.A. (1994) The Epstein-Barr virus (EBV) small RNA EBER1 binds and relocalises ribosomal protein L22 in EBV-infected human B lymphocytes. *Proc. Natl Acad. Sci. USA*, **91**, 3463–3467.

Trayer,I.P. and Smith,J.K. (1997) Motoring down the highways of the cell. *Trends Cell Biol.*, **7**, 259–263.

Vernos,I., Raats,J., Hirano,T., Heasman,J., Karsenti,E. and Wylie,C. (1995) Xklp1, a chromosomal *Xenopus* kinesin-like protein essential for spindle organization and chromosome positioning. *Cell*, **81**, 117–127.

Walczak,C.E. and Mitchison,T.J. (1996) Kinesin-related proteins at mitotic spindle poles: function and regulation. *Cell*, **85**, 943–946.

Walczak,C.E., Mitchison,T.J. and Desai,A. (1996) XKCM1: a *Xenopus* kinesin-related protein that regulates microtubule dynamics during mitotic spindle assembly. *Cell*, **84**, 37–47.

Ward,D.M., Leslie,J.D. and Kaplan,J. (1997) Homotypic lysosome fusion in macrophages: analysis using an *in vitro* assay. *J. Cell Biol.*, **139**, 665–673.

Wordeman,L. and Mitchison,T. (1995) Identification and partial characterisation of mitotic centromere-associated kinesin, a kinesin-related protein that associates with centromeres during mitosis. *J. Cell Biol.*, **128**, 95–104.

Yamazaki,H., Nakata,T., Okada.,Y. and Hirokawa,N. (1995) KIF3A/B: a heterodimeric kinesin superfamily protein that works as a microtubule plus end-directed motor for membrane organelle transport. *J. Cell Biol.*, **130**, 1387–1399.

Yamazaki,H., Nakata,T., Okada.,Y. and Hirokawa,N. (1996) Cloning and characterisation of KAP3: a novel kinesin superfamily-associated protein of KIF3A/3B. *Proc. Natl Acad. Sci. USA*, **93**, 8443–8448.

*Received April 7, 1998; revised August 18, 1998; accepted August 19, 1998*